

RESEARCH

Open Access



Epidemiological investigation and analysis of the infection of porcine circovirus in Xinjiang

Kai Yang^{1†}, Zunbao Wang^{1,2†}, Xinyu Wang¹, Mingfang Bi¹, Suhua Hu¹, Kaijie Li¹, Xiaomei Pan², Yuan Wang², Dan Ma¹ and Xiaobing Mo^{1*}

Abstract

Porcine circoviruses, particularly porcine circovirus type 2 (PCV2) and porcine circovirus type 3 (PCV3), significantly impact the global pig industry due to their high prevalence and pathogenicity. Conversely, porcine circovirus type 1 (PCV1) and porcine circovirus type 4 (PCV4) currently have low positivity rates. This study aimed to characterize the distribution and epidemiology of porcine circoviruses in Xinjiang, while also analyzing the genetic diversity and evolution of PCV2 and PCV3, which pose the greatest threats to the industry. In this study, we collected blood and tissue samples from 453 deceased pigs across eight regions in Xinjiang Province from 2022 to 2024. We utilized real-time PCR to detect the presence of PCV1, PCV2, PCV3, and PCV4. The positive rates were 15%, 71%, 25%, and 17%, respectively. Genetic analysis showed 9 PCV2 sequences and 12 PCV3 sequences. The capsid protein of PCV2 showed significant variability. In contrast, the amino acid sequences of capsid in PCV3 were relatively stable. Moreover, we predicted antigenic epitopes for PCV3 capsid using IEDB and ElliPro. The findings from this study provide valuable epidemiological data on PCV coinfection in the Xinjiang region and enhance the understanding of virus diversity nationwide. This research may serve as an important reference for the development of strategies to prevent and control porcine circovirus infections.

Keywords Porcine circovirus, Epidemiological investigation, Xinjiang, Phylogenetic analysis

Introduction

Circoviruses comprise a family of viruses characterized by the smallest known viral genomes consisting of circular single-stranded DNA. These viruses are prevalent across a wide range of hosts including humans, birds, pigs, bats, and other animals. Porcine circoviruses (PCVs) are categorized into four distinct types based on the order of their discovery: porcine circovirus type

1 (PCV1), Porcine circovirus type 2 (PCV2), porcine circovirus type 3 (PCV3), and porcine circovirus type 4 (PCV4) [1]. PCV1, first identified in the porcine kidney cell line 15 (PK-15), has a genome approximately 1760 nucleotides (nt) in length and is generally regarded as non-pathogenic, often considered a contaminant in biological materials [2, 3]. Conversely, PCV2, identified in 1998, has emerged as a major pathogen in the global pig industry, with a genome of about 1700 nt [4]. It is differentiated into eight genotypes (2a, 2b, 2c, 2d, 2e, 2f, 2 g and 2 h) based on the DNA sequence variations in the open reading frame 2 (ORF2) [5–9]. It is known that mixed infections of PCV2 and other pathogenic microorganisms can lead to a series of diseases, including post-weaning multisystemic wasting syndrome (PMWS), porcine dermatitis and nephropathy syndrome (PDNS), respiratory diseases, congenital tremors, and

[†]Kai Yang and Zunbao Wang have made equal contributions to this research.

*Correspondence:
Xiaobing Mo
mox@jlu.edu.cn

¹ College of Veterinary Medicine, State Key Laboratory for Diagnosis and Treatment of Severe Zoonotic Infectious Diseases, Key Laboratory for Zoonosis Research of the Ministry of Education, Institute of Zoonosis, Jilin University, Changchun 130062, China

² Tecon Pharmaceutical Co., Ltd, Ürümqi 830000, China



reproductive problems [10–12]. PCV3, discovered in 2016 in the United States, has a genome of about 2000 nt and is subdivided into three genotypes (PCV3a, PCV3b, and PCV3c), distinguished by variations in the capsid of PCV3 [13, 14]. When co-infected with other pathogens, it is associated with similar clinical symptoms as co-infection with PCV2, such as respiratory failure, encephalitis, myocarditis, abortion and fetal mummification, in addition to PDNS [15, 16]. PCV4 was first detected in Hunan Province, China, in 2019 in a pig also infected with African swine fever, presenting severe clinical signs. Its genome, approximately 1770 nt in size, shows 43.2–51.5% similarity with other porcine circoviruses. To date, the association of PCV4 with specific clinical symptoms remains unclear [17]. Epidemiological data reveal variable prevalence rates across different regions in China: PCV1 exhibits a prevalence of 4.17% in Jiangsu. Investigations in Shanxi and Henan indicated PCV2 and PCV3 positivity rates of 57.07% and 36.36%, respectively [18, 19]. Southern China showed a PCV2 positivity rate of 69.5%, in a 2018–2019 survey in Henan, PCV2 and PCV3 were detected at rates of 72.9% and 5.17%, respectively [9, 20]. The detection rates for PCV4 are 3.33% in Jiangsu and 5.05% in Guangxi [17, 21].

Xinjiang, encompassing approximately one-sixth of China's total land area, hosts a notable pig population and has witnessed steady growth in its animal husbandry sector in recent years. Given its unique geographical and ecological attributes, Xinjiang offers diverse natural conditions conducive to studying the epidemiological characteristics of porcine circoviruses (PCVs). This underscores the importance of conducting comprehensive epidemiological investigations and evolutionary analyses of PCVs in the region. A previous study recorded a PCV3 positivity rate of 22.39% in Xinjiang in 2019 [22]. Despite this, there remains a paucity of data on the current epidemic trends and an absence of detailed analysis on the infections and co-infections involving PCV1, PCV2, and PCV4.

In our study, we examined samples from 453 diseased pigs across 22 farms in 8 different areas of Xinjiang, spanning from 2022 to 2024. The goal was to elucidate the infection statuses and distribution patterns of PCV1 through PCV4, and to perform an epidemiological analysis on these viruses. Additionally, we conducted genetic analyses on the ORF2 genes of PCV2 and PCV3 to assess the genetic variations and evolutionary dynamics of the capsid protein in these viruses.

Methods

The collection of clinical samples

From August 2022 to January 2024, a total of 453 clinical samples were collected from diseased pigs across 22 farms situated in 8 different regions of Xinjiang. The sample types included blood, lung, liver, and lymph nodes. The affected pigs exhibited symptoms that varied in severity, encompassing respiratory distress, reproductive issues, and severe emaciation due to diarrhea. The geographical breakdown of the sample collection was as follows: AKeSu (48), Changji (48), HaMi (72), KaShi (18), BaYin (48), ShiHeZi (99), WuJiaQu (36), and YiLi (84). The pigs sampled ranged across different developmental stages from conservation, through pregnancy, to fattening. Each sample was uniquely collected from individual pigs.

The extraction of DNA from the samples

For blood samples, 200 μ L were drawn, and genomic DNA was extracted following the protocol provided by the YALEPIC[®] Universal Genomic DNA Isolation Kit (YALI, China). For tissue samples, 25 mg was harvested, finely minced, and subsequently pulverized using liquid nitrogen, in preparation for DNA extraction as per the kit guidelines. The extracted DNA was then preserved at -80°C . PCV1–PCV4 positive plasmids (Tecon, Xinjiang) were used as detection controls.

The detection and analysis of PCVs

The nucleic acids of PCVs were detected using a SYBR Green-based quantitative PCR (qPCR) method. The reaction mixture comprised 10 μ L of $2 \times$ M5 HiPer SYBR Premix EsTaq (with Tli RNaseH) (Mei5bio, China), 0.4 μ L of each specific primer (Supplementary Table 4), 0.4 μ L of ROX Reference Dye II (50 \times), and 2 μ L of DNA template. The volume was adjusted to 20 μ L with nuclease-free water. The qPCR cycling parameters on the QuantStudio 3 Real-time PCR system (Thermo, USA) were set as follows: initial denaturation at 95°C for 10 min, followed by 40 cycles of denaturation at 95°C for 30 s, annealing at 60°C for 30 s, and extension at 72°C for 30 s with fluorescence data collection. To ensure the reliability of the detection, positive and negative controls were included, and a subset of the 453 positive samples were randomly selected for sequencing verification. The infection data was visualized using Chiplot and the Venn diagram was drawn using jvenn [23]. Geographical analysis of PCVs was visualized using DataV (https://datav.aliyun.com/portal/school/atlas/area_selector) and Adobe Illustrator 2022.

Amplification, cloning, and evolutionary analysis of the ORF2 gene

The ORF2 sequences of PCV2 and PCV3 were amplified using primers detailed in Supplementary Tables 4, and the resultant DNA fragments were cloned into the pUC57 vector and sequenced by Sangon(Shanghai, China). The acquired sequences were aligned and compared with reference sequences from the NCBI database (Supplementary Tables 4 and 4) using MEGA 11.0 software under default parameters. The most suitable Bayesian model for phylogenetic analysis was identified via MEGA 11.0, and an evolutionary tree was constructed using the maximum likelihood (ML) approach with the GTR+G+I model, supported by 1000 bootstrap replicates. Additionally, the amino acid

sequences of the capsid protein for both PCV2 and PCV3 were analyzed in DNAMAN. Antigenic epitopes of the PCV3 capsid protein were predicted using tools from IEDB and ElliPro. The findings were visualized using GraphPad Prism 9 and PYMOL software for detailed graphical representation.

Results

Prevalence of PCVs in Xinjiang of China

In the study conducted in Xinjiang, China, data analysis from a total of 453 samples indicated distinct infection rates for porcine circoviruses (Table 1). Specifically, the positive rates for PCV1, PCV2, PCV3, and PCV4 were found to be 15%, 71%, 25%, and 17%, respectively (Fig. 1a). Moreover, the rates of mixed infections were analyzed as

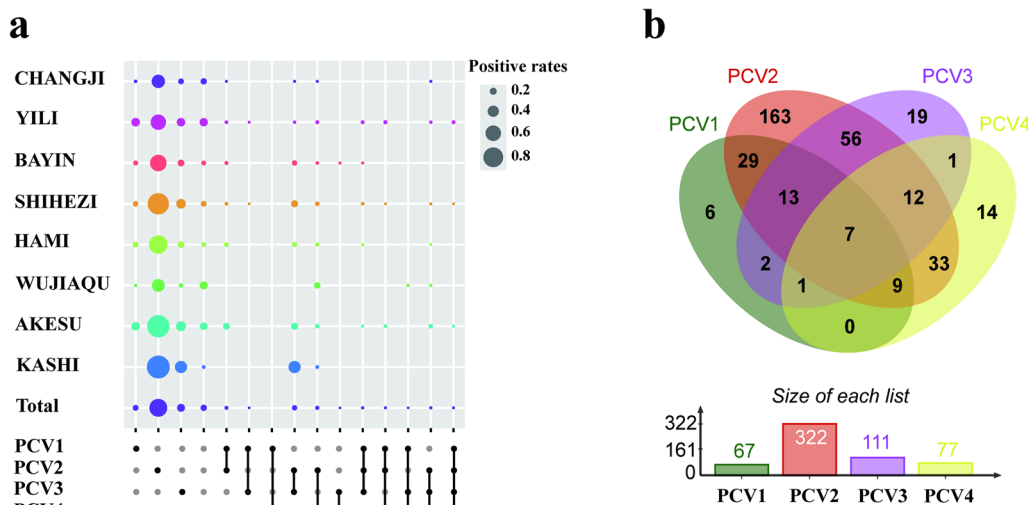


Fig. 1 Prevalence of PCVs in Xinjiang of China **a** The image presents a heatmap depicting the prevalence of PCV infections across various regions in Xinjiang. Black dots and lines specify the type of infection present, while the relative size of the circles indicates the intensity of the infection in each region. **b** The Venn diagram illustrates detailed information on mixed infections, while the bar chart provides granular data regarding individual infection types and their frequencies

Table 1 The prevalence of PCVs in different regions in Xinjiang of China

City	Samples (n)	PCV1 positive (n)	PCV1 prevalence (%)	PCV2 positive (n)	PCV2 prevalence (%)	PCV3 positive (n)	PCV3 prevalence (%)	PCV4 positive (n)	PCV4 prevalence (%)
AKeSu	48	13	27.1	44	91.7	16	33.3	11	22.9
Changji	48	2	4.2	24	50.0	7	14.6	8	16.7
HaMi	72	10	13.9	53	73.6	13	18.1	7	9.7
KaShi	18	0	0	17	94.4	8	44.4	1	5.6
BaYin	48	5	10.4	31	64.6	9	18.8	5	10.4
YiLi	84	23	27.4	50	59.5	23	27.4	22	26.2
ShiHeZi	99	13	13.1	86	86.9	32	32.3	14	14.1
WuJiaQu	36	1	2.8	17	47.2	3	8.3	9	25.0
Total	453	67	14.8	322	71.1	111	24.5	77	17.0

follows: 6.4% for co-infections of PCV1 and PCV2; 0.44% for PCV1 and PCV3; none for PCV1 and PCV4; 12.36% for PCV2 and PCV3; 7.28% for PCV2 and PCV4; 0.22% for PCV3 and PCV4; 2.87% for tri-infections involving PCV1, PCV2, and PCV3; 1.99% for PCV1, PCV2, and PCV4; 0.22% for PCV1, PCV3, and PCV4; 2.65% for PCV2, PCV3, and PCV4; and 1.55% for infections of PCV1, PCV2, and PCV3, and PCV4 (Fig. 1b). Notably, the overall infection rate of PCV2 was relatively high, with the highest mixed infection rate observed between PCV2 and PCV3. In contrast, the infection rates for both PCV1 and PCV4 were comparatively lower (Fig. 1b).

Geographical distribution of PCVs

In eight regions of Xinjiang, diverse strains of porcine circoviruses (PCVs) were detected, with notable variations in their prevalence, except for Kashi where PCV1 was not detected. Among these regions, Yili

exhibited the highest infection rate of PCV1 at 27.4%, contrasting with Kashi where PCV1 was absent. Conversely, Kashi demonstrated the highest positive rate for PCV2 at 94.4%, followed by Aksu at 91.7% and Shihezi at 86.9%, while Wujiaqu exhibited the lowest infection rate at 47.2%. Regarding PCV3, Kashi showed the highest infection rate at 44.4%, followed by Aksu at 33.3%, with Wujiaqu recording the lowest rate at 8.3%. In terms of PCV4, Yili had the highest infection rate at 26.2%, whereas Kashi exhibited the lowest at 5.6% (Table 1). Geospatial distribution analysis reveals that among the 8 surveyed regions, PCV1 was not detected in the KaShi region, while PCV1 to PCV4 were detected in the remaining regions (Fig. 2a–d). PCV1 and PCV4 were predominantly distributed in western Xinjiang, while PCV2 was prevalent in the southwest and northeast regions (Fig. 2a, b and d). PCV3 exhibited

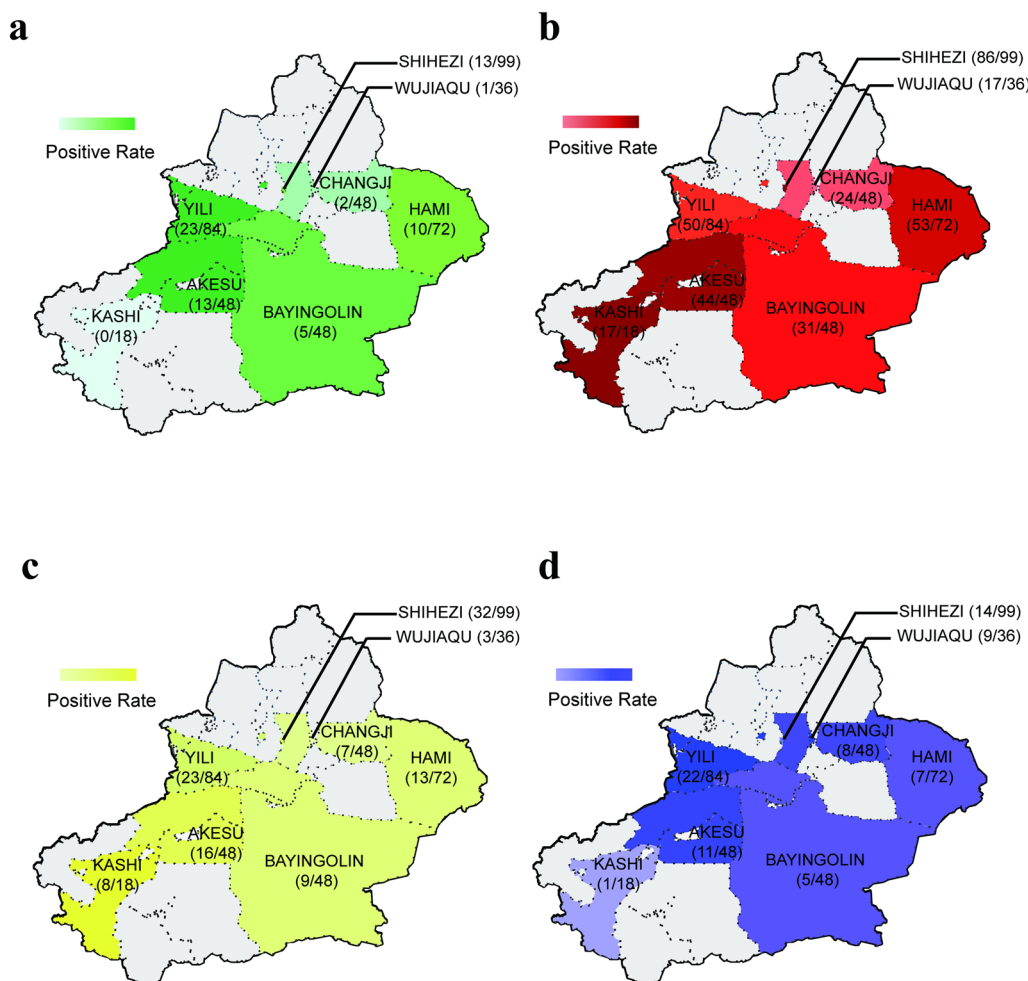


Fig. 2 Geographic visualization of PCV infection status **a** The visualization captures the infection status of PCV1 across Xinjiang. **b** The depiction shows the prevalence of PCV2 infections throughout Xinjiang. **c** The graphic represents the distribution of PCV3 infections across the region of Xinjiang. **d** The image illustrates the infection status of PCV4 in Xinjiang

a higher positivity rate in the southwestern region of Xinjiang (Fig. 2c).

Molecular characterization of PCV2

The ORF2 gene of nine PCV2 strains were sequenced, and their sequences submitted to GenBank at National Center for Biotechnology Information (NCBI), where corresponding accession numbers were recorded (Table 2). For comparative analysis, gene sequences of 25 representative PCV2 ORF2 genes with distinct subtypes were retrieved from the NCBI database (Supplementary Table 1). These sequences facilitated the construction of the evolutionary tree for ORF2 (Fig. 3a). According to this phylogenetic analysis, the nine sequences comprised one PCV2e, four PCV2b, and four PCV2d strains.

To further examine variations in the capsid protein, which carries major immunogenic properties, sequences from three vaccine strains and 28 reference strains were aligned for amino acids comparison. Critical epitopes previously identified include the regions spanning amino acids 51–81, 113–139, 161–208, 227–233, and the immunodominant bait epitope 168–180 [24–27]. Previous studies have highlighted that the N-terminal NLS segment of the PCV2 capsid protein functions as a cell-penetrating

peptide, significantly impacting viral infection dynamics in cells. The core epitopes of the NLS include NLS-A (MTYPRRRFRRRRHRPRS) and NLS-B (QILRRRPWLHPRHRYRWRRK), situated at amino acid positions 1–17 and 27–41, respectively [28, 29]. Notably, when compared to other different isoforms, PCV2b has undergone mutations in four amino acids, three of which (Lys⁵⁹, Arg⁶³, and Thr¹⁰⁹) were located at antigen recognition sites, and one (Ile³⁰) at the NLS-B site. PCV2d strains exhibited three amino acid mutations relative to other different isoforms, all located within the antigen recognition region (Ser¹⁶⁹, Lys¹⁸⁰, and Lys²³²), with two (Ser¹⁶⁹ and Lys¹⁸⁰) positioned at critical antigenic epitope sites. The newly sequenced PCV2e strain showed two amino acid mutations relative to same isoforms, one of which (Asn¹²⁷) was within the antigen recognition area. Significant differences were observed in the antigenic epitopes between PCV2e and the predominant PCV2d strain (Supplementary Fig. 1). Nucleotide similarity among the nine ORF2 sequences ranged from 92.4 to 94.8% between PCV2b and PCV2d, from 81.8 to 84.0% between PCV2b and PCV2e, and from 84.2 to 84.5% between PCV2d and PCV2e. These observations align with findings from previous research [30].

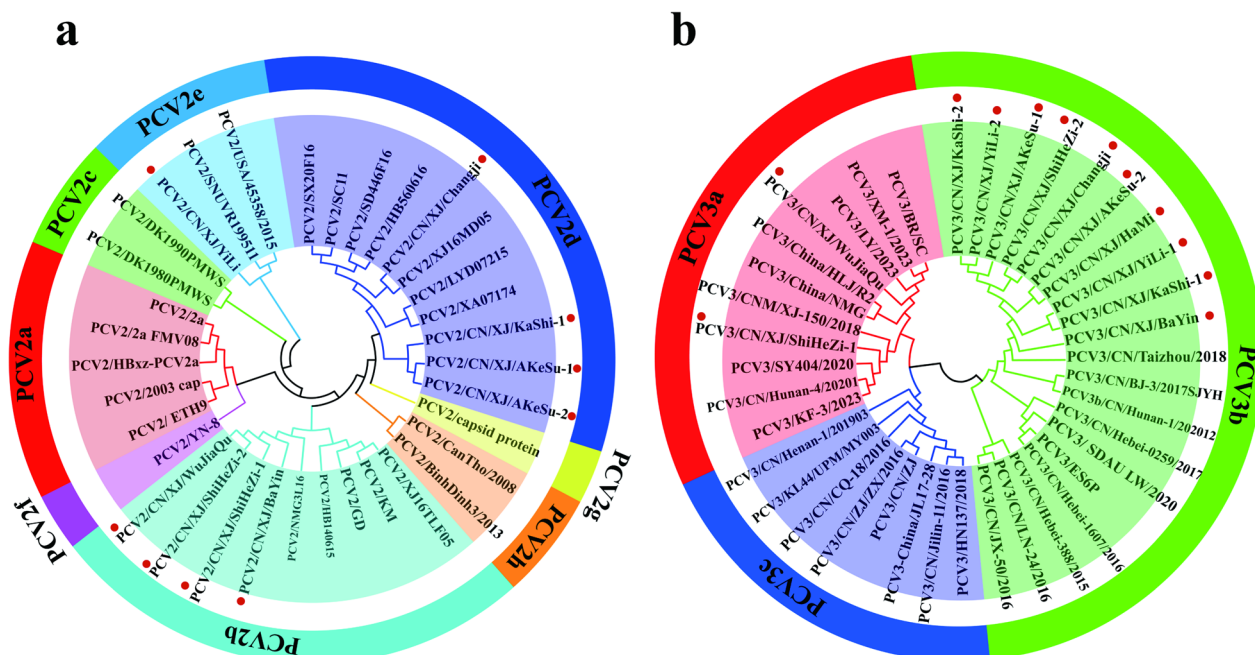


Fig. 3 Constructing evolutionary trees based on ORF2 for PCV2 and PCV3 **a** This figure displays an evolutionary tree alongside genotyping for 9 PCV2 ORF2 sequences derived from this study, compared with 25 PCV2 ORF2 sequences sourced from the NCBI database. Different genotypes are indicated by various colors, with red dots highlighting the sequences obtained in our study. **b** It illustrates an evolutionary tree and genotyping for 12 PCV3 ORF2 sequences acquired from this research, alongside 27 PCV3 ORF2 sequences from NCBI. Various genotypes are depicted in distinct colors, with sequences from this investigation represented by red dots

Table 2 The information of PCV2 and PCV3 strains sequenced in this study

Strain	Collection data	Location	Accession number	Genotype
PCV2/BaYin	2022.10.27	BaYin	PP707852	PCV2b
PCV2/ShiHeZi-1	2022.12.15	ShiHeZi	PP707853	PCV2b
PCV2/ShiHeZi-2	2023.04.05	ShiHeZi	PP707854	PCV2b
PCV2/WuJiaQu	2023.07.21	WuJiaQu	PP707855	PCV2b
PCV2/Changji	2022.11.11	Changji	PP707856	PCV2d
PCV2/KaShi-1	2023.02.07	KaShi	PP707857	PCV2d
PCV2/AKeSu-1	2023.03.15	AKeSu	PP707858	PCV2d
PCV2/AKeSu-2	2023.08.21	AKeSu	PP707859	PCV2d
PCV2/YiLi	2023.07.17	YiLi	PP707860	PCV2e
PCV3/ShiHeZi-1	2022.11.05	ShiHeZi	PP707861	PCV3a
PCV3/WuJiaQu	2023.06.22	WuJiaQu	PP707862	PCV3a
PCV3/KaShi-2	2022.12.05	KaShi	PP707863	PCV3b
PCV3/YiLi-2	2023.01.17	YiLi	PP707864	PCV3b
PCV3/AKeSu-1	2022.10.11	AKeSu	PP707865	PCV3b
PCV3/ShiHeZi-2	2023.03.16	ShiHeZi	PP707866	PCV3b
PCV3/Changji	2023.09.23	Changji	PP707867	PCV3b
PCV3/AKeSu-2	2023.07.11	AKeSu	PP707868	PCV3b
PCV3/HaMi	2023.08.22	HaMi	PP707869	PCV3b
PCV3/YiLi-1	2023.12.07	YiLi	PP707870	PCV3b
PCV3/KaShi-1	2023.04.25	KaShi	PP707871	PCV3b
PCV3/BaYin	2023.10.13	BaYin	PP707872	PCV3b

Molecular characterization of PCV3

For comparative analysis, gene sequences of 27 PCV3 ORF2 gene obtained from NCBI were utilized (Supplementary Table 2). These sequences were employed to construct the evolutionary tree for ORF2 (Fig. 3b). The phylogenetic analysis identified two of the 12 sequences as PCV3a and the remaining ten as PCV3b. Nucleotide similarity among the 12 ORF2 gene sequences of PCV3a and PCV3b ranged from 95.5 to 97.1%. To further explore the mutation status of the capsid protein, known for its significant immunogenic properties, amino acid alignment was performed using DNAMAN, which revealed that the PCV3a (ShiHeZi-1) strain exhibited three amino acid mutations (Thr⁶¹, Phe⁸⁸, and Leu¹³⁴) relative to other different isoforms, while the PCV3b strains displayed four amino acid mutations relative to other different isoforms (Thr⁶¹, Asn¹⁹⁵, Arg¹⁹⁶, and Phe¹⁹⁷) (Supplementary Fig. 2).

PCV3 capsid antigenic epitope prediction

After sequence comparison using DNAMAN, the amino acid sequences of PCV3 capsid protein were found to be highly conserved (Supplementary Fig. 2). Consequently, the strain PCV3/KaShi-2 was selected for antigenic epitope prediction using the IEDB platform. The Kolaskar and Tongaonkar antigenicity model, which has a prediction accuracy of 75% [31], was employed to identify

potential conserved epitopes that could inform the development of vaccines with broader antigenic coverage. This model has previously been used for antigenic epitope prediction in dengue virus and influenza A [32, 33]. The Kolaskar and Tongaonkar antigenicity prediction method identified five antigenic peptides ranging from 7 to 21 amino acids in length within the 197 amino acid sequence, with the longest peptide measuring 21 amino acids and achieving a score of 1.076 (Supplementary Table 3). The relationship between potential conserved epitopes and the amino acid residues of the PCV3 capsid protein is depicted in Fig. 4a, with an average score of 1.009 (minimum: 0.881; maximum: 1.165). Additionally, the Chou and Fasman Beta-Turn Prediction model was used to predict beta-turns in the protein structure, known to likely be exposed on protein surfaces and thus possessing potential immunogenicity [34, 35]. Beta-turn structures, which are often exposed on protein surfaces and targeted by the immune system, were predicted using Chou and Fasman beta-turn prediction; peptides, GTPQNNK (a.a 36–42), TPQNNKP (a.a 37–43), and PQNNKPW (a.a 38–44), showed higher propensities for forming beta-turns with scores around 1.301 (Fig. 4b). Surface accessibility was assessed using the Emini surface accessibility prediction, this model is well-established and widely used in immunological studies [34, 36]. The Emini surface accessibility prediction indicated high surface

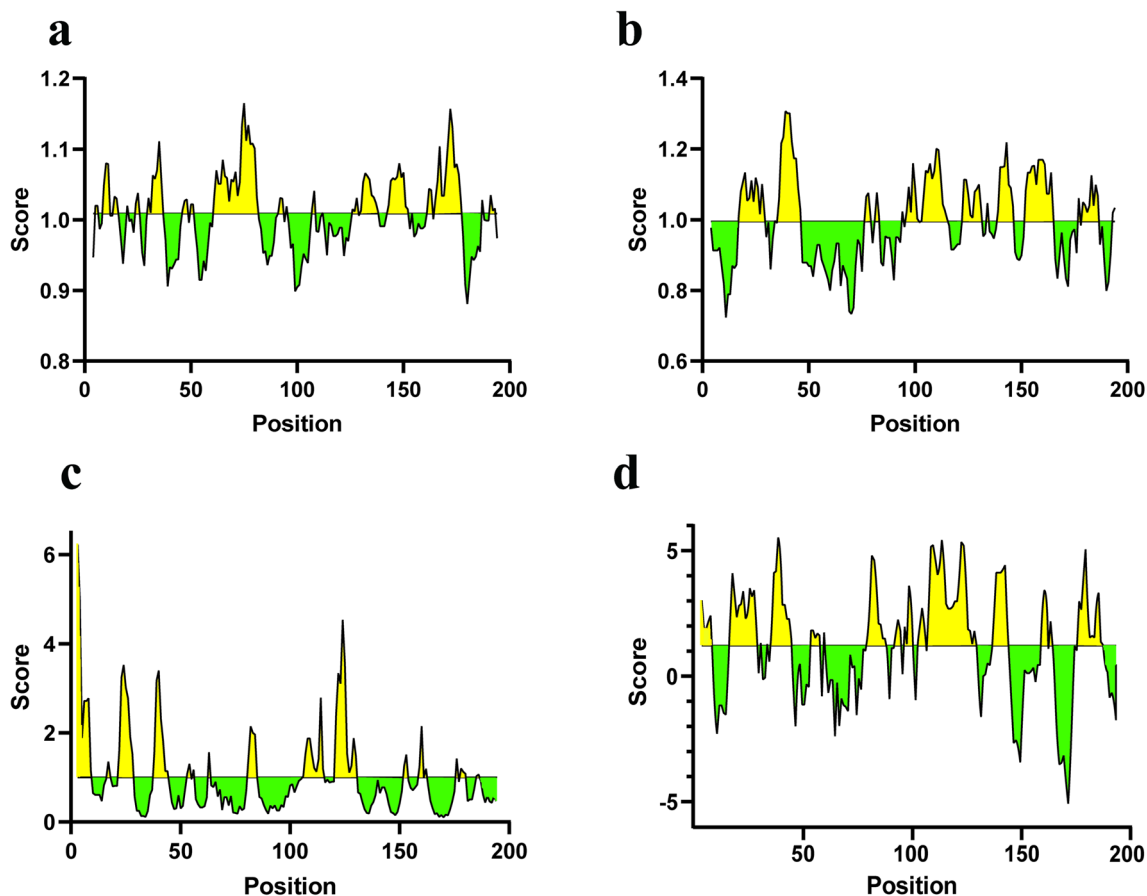


Fig. 4 Prediction of linear epitopes of PCV3 Capsid using IEDB **a** Depiction of potential antigenic conserved sites within PCV3 Capsid protein using the Kolaskar and Tongaonkar antigenicity scale (Threshold = 1.009). **b** Illustration of the secondary structure of the protein employing the Chou and Fasman Beta-Turn prediction model, highlighting β -turn epitopes which are likely more exposed on the protein surface (Threshold = 0.995). **c** Diagram predicting the surface accessibility of the Capsid protein using the Emini surface accessibility prediction method (Threshold = 1.000). **d** Visualization of the protein surface hydrophilicity using the Parker Hydrophilicity prediction model (Threshold = 1.227). Yellow regions indicate predicted favorable areas, while green regions denote less favorable areas

accessibility for SKKKHSRYFT (a.a 121–130), suggesting their likelihood of exposure to solvents or antibodies, while QDDPYAESST (a.a 106–115) exhibited a markedly lower score of 2.624 (Fig. 4c). The Parker hydrophilicity prediction was applied to determine regions of the capsid protein that are hydrophilic and therefore likely to interact more readily with antibodies, enhancing immune recognition [37]. Hydrophilicity, as assessed by the Parker hydrophilicity prediction, highlighted the TWLQDDPYAESSTRKVMTSKKHSRYFT segment (a.a 103–130) as having a high hydrophilicity score of 2.696, indicating enhanced solubility (Fig. 4d). The Karplus and Schulz flexibility prediction model focused on predicting the flexibility of protein chains, crucial for determining the structural and functional properties of proteins, underscoring its potential importance in clinical diagnostic and vaccine development strategies due to its structural dynamics [38–40]. Protein flexibility

was evaluated using The Karplus and Schulz flexibility prediction, with residue Asn⁴⁰ in the TPQNNKP segment (a.a 37–43) showing the highest flexibility score of 1.111 (Fig. 5a). Additionally, BepiPred Linear Epitope Prediction 2.0, a tool designed specifically for predicting linear B-cell epitopes [41], . BepiPred Linear Epitope Prediction 2.0 identified potential B cell epitope sites in the capsid protein, with ISPAQQTMTMFG segments (a.a 78–89) and AWTTNTWLQDDPYAESSTRKVMTS KKKHSRYFT (a.a 98–130) scoring below the threshold, contrasting with the higher scoring RRYVRRKLFIRRPPT segment (a.a 5–18) (Fig. 5b). According to Supplementary Table 3, the YYTKKYS segment (a.a 22–28) met all four screening criteria, marking it as a likely potential antigenic epitope, and the amino acid comparison chart confirmed this region's conservation (Supplementary Fig. 2). Previously identified linear B cell antigenic epitopes of PCV3 capsid (KHSRYFT, NKPWH,

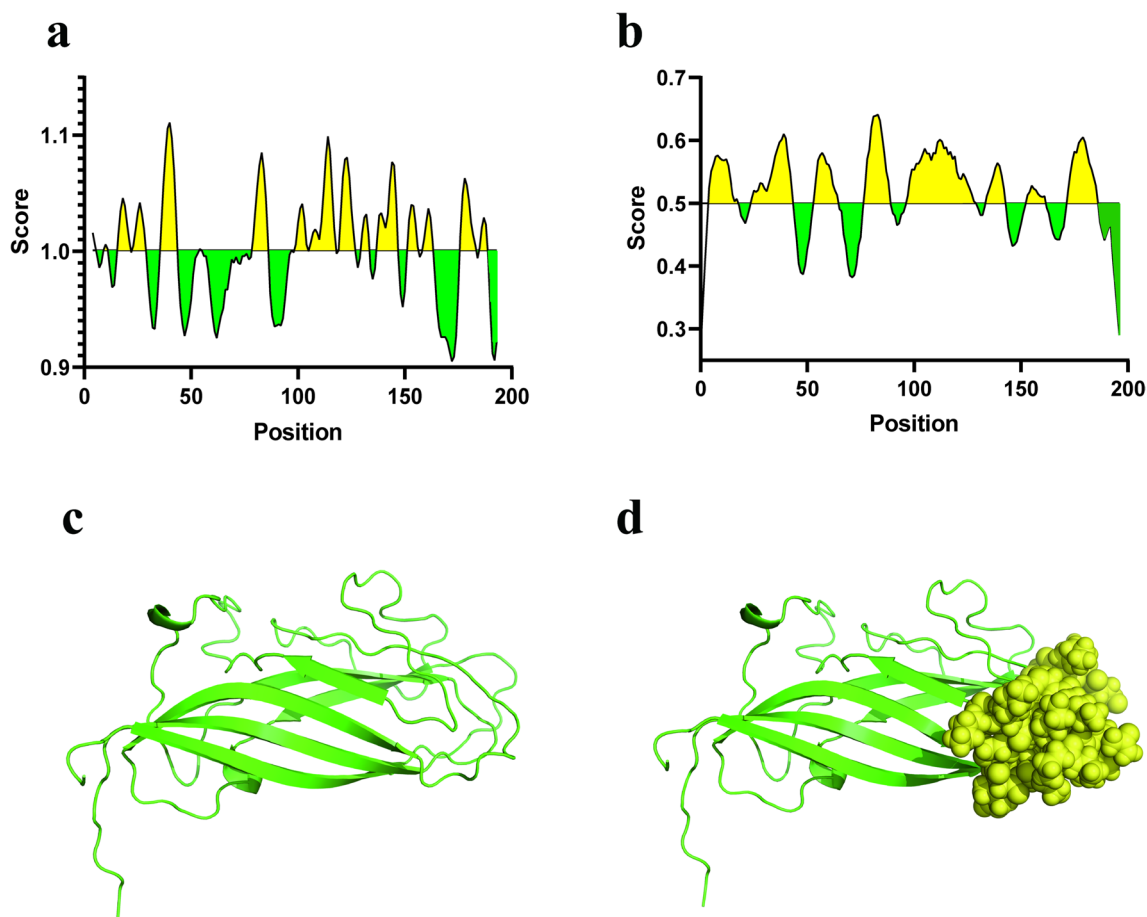


Fig. 5 Prediction of linear and discontinuous epitopes of PCV3 capsid **a** Assessment of capsid protein flexibility employing the Karplus and Schulz method (Threshold=1.001). **b** Prediction of linear B-cell epitopes within the protein sequence utilizing BepiPred linear epitope prediction 2.0 (Threshold=0.500). **c** Rendering of the PCV3 capsid structure in 3D using PYMOL. **d** Identification of discontinuous epitopes situated in the loop region via ElliPro. The green cartoon linear sections represent the 3D rendered model of the PCV3 capsid structure using PyMOL. The yellow spherical structures indicate the discontinuous epitope regions located in the Loop areas identified by ElliPro, presented in a visual format

WLQDDPYAESSTRKV) (Supplementary Table 3) were all found to have high scores on the four scoring methods, which is consistent with the verification results [42, 43].

Predicted structural epitopes of PCV3 capsid

ElliPro employs the protrusion index, derived from the analysis of resolved protein structures, to predict discontinuous epitopes within the three-dimensional configuration of antibody-antigen complexes. This approach surpasses traditional linear epitope prediction techniques in accuracy for identifying antibody epitopes [44]. We utilized the three-dimensional (3D) structure of the PCV3 capsid protein crystal, previously resolved by Cryo-EM in our laboratory (Supplementary File 1) [45], to predict epitopes using the ElliPro tool. The results identified one discontinuous epitope on the structural surface of the protein with a score exceeding 0.7

(Fig. 5c–d). Detailed information regarding the location, number of residues involved, and the scoring of this predicted epitope is presented in Table 3.

Discussion

The prevalence of porcine circoviruses (PCVs), specifically PCV1, PCV2, PCV3 and PCV4, have been extensively reported across China. Notably, the positive detection rate for PCV1 in the Jiangsu region stands at 4.17% [18]. Investigations in Shanxi and Henan regions have revealed positive rates of 57.07% for PCV2 and 36.36% for PCV3, respectively [19]. In Southern China, the positivity rate for PCV2 has reached 69.5% [20]. Further, epidemiological data from Henan between 2018 and 2019 indicate positivity rates of 72.9% for PCV2 and 5.17% for PCV3 [9], whereas a similar survey in Tianjin from 2018 to 2020 showed positivity rates of approximately 57% for PCV2, 37%

Table 3 The location, number of residues, and score of the predicted results using ElliPro

Residues and positions	Number of residues	Score	3D structure
V35, G36, T37, P38, Q39, N40, N41, K42, P43, P76, V77, I78, S79, P80, A81, Q82, Q83, T84, K85, T86, S121, K122, K123, K124, W171, S172, I173, Y174, E177	29	0.736	Figure 5d

for PCV3, and a co-infection rate of 20% for both viruses [46]. In Xinjiang, a 2019 study reported a PCV3 positivity rate of 22.39% [22]. The infection rates for PCV4 in the Jiangsu and Guangxi areas were reported at 3.33% and 5.05%, respectively [17, 21]. In Henan, out of 30 pig farms surveyed, the positivity rates were approximately 64% for PCV2 and 33% for PCV4, with a co-infection rate of about 21% [47]. The epidemiological survey results from previous studies indicate that PCV2 and PCV3 have generally high positivity rates across various regions in China, while PCV1 and PCV4 have lower positivity rates. This is consistent with the epidemiological findings of this study focused on the region of Xinjiang, China. The positive rate of PCV2 is the highest, with PCV3 ranking second, while the positive rates of PCV1 and PCV4 are at lower levels. The study found that mixed infections of PCVs in the Xinjiang region were predominantly co-infections of PCV2 and PCV3. From the perspective of co-infections with other viruses, previous studies have shown that PCV2 and PCV3 are primarily involved in mixed infections with other viruses. In the lungs, other pathogens co-infecting with PCVs include porcine reproductive and respiratory syndrome virus (PRRSV), swine influenza virus (SIV), and mycoplasma hyopneumoniae (MHP). Co-infection of PCVs and porcine parvovirus (PPV) enhances the symptoms of postweaning multisystemic wasting syndrome. In sows and aborted fetuses, PCVs can primarily occur as mixed infections with PPV, PRRSV, and other viruses [48]. When researchers compared the virulence of a single subtype versus all four subtypes co-infected with PRRSV, they found that PCV2d was the most virulent PCV2 subtype in pigs co-infected with PRRSV. PRRSV can affect the infection dynamics of PCV2a and PCV2b subtypes by enhancing PCV2 viremia and delaying viral shedding in the body [49]. Furthermore, co-infection with different PCV2 genotypes may lead to more severe disease. In cells infected with replicating viruses, both PCV2a and PCV2b genotypes are present [50]. Further studies have shown that pigs naturally infected with multiple PCV2 genotypes or strains exhibit more severe lesions [51, 52]. Co-infection with classical swine fever virus (CSFV), PRRSV, and PCVs not only leads to more severe disease than single infections [53], but also negatively impacts immune responses [54].

PPV and PCV2 play important roles in reproductive disorders of sows. PPV infection provides a better in vivo environment for PCV2 infection [48]. SIV does not affect PCV2 virus replication in co-infected pigs, but PCV2 infection increases SIV-related clinical disease [55, 56]. The PEDV genomic RNA levels in sows co-infected with PEDV and PCV2 were significantly lower than in sows infected with PEDV alone. This may be due to PEDV's rapid replication in the early stages of infection, which destroys villous intestinal cells. This results in a significant reduction of cells available for PEDV replication in the later stages of infection [57]. Currently, large-scale farms in the Xinjiang region are still under the infection pressure from PCV2 and PCV3. Different PCVs also exhibit distinct geographical distributions. The highly pathogenic PCV2 and PCV3 are both present in the southwestern regions, which may be attributed to the distribution of large-scale farms in different areas or variations in biosecurity strategies. In the year 2000, the predominant genotype of PCV2 worldwide was identified as PCV2a [58]. Subsequently, genetic evolution led to the emergence of PCV2b as the dominant strain due to genetic drift [59–61]. The continuous evolutionary dynamics of PCV2 may be influenced by vaccination, leading to coexistence of PCV2b and PCV2d variants [59, 62–64]. Currently, in the Xinjiang region, the main subtypes of PCV2 are primarily 2b and 2d, and these two subtypes remain the primary targets for future prevention, control, and immunization efforts. Geographically speaking, the differences in PCV2b and PCV2d across various regions may be due to the import and export of animals between different areas, as well as variations in vaccine types and strategies. Temporally, PCV2b was mainly detected in 2022, while PCV2d and PCV2e were predominantly detected in 2023, which might be attributed to the evolutionary pressure exerted by the selective use of PCV2b vaccines, leading to a gradual evolution towards PCV2d and PCV2e. Mutations at critical sites in PCV2b and PCV2d may lead to immune escape from the existing vaccines. The YiLi strain could represent a novel variant with potential immune escape capabilities against current vaccines, which may also alter its virulence [65]. The capsid protein's recognition and induction regions are

critical for viral replication and immune evasion in the host [66–68]. For PCV3, the predominant strain in 2022 and 2023 is PCV3b. However, within the same isoform and across different isoforms, PCV3b exhibits fewer amino acid mutation sites and is overall more conserved. This conservatism may be due to the absence of a suitable vaccine, which has resulted in a slower rate of viral evolution. Mutations in these key areas may compromise antibody recognition, potentially rendering existing vaccines ineffective and facilitating widespread viral transmission within pig populations, promoting further genetic variability [69]. Despite the availability of several vaccines, the persistence and high mutation rate of PCV2 continue to challenge control efforts [70]. The mutation site information obtained from this evolutionary analysis of the PCV2 Capsid protein will be beneficial for the subsequent design and improvement of vaccines. Further analysis using identified the peptide sequence ‘YYTKKYS’ (a.a 22–28) as a potential linear antigenic epitope for PCV3, exceeding the model’s threshold and meeting the prediction criteria for a promising candidate in PCV3 diagnostics or vaccine design [41]. In the current study, ElliPro successfully predicted a discontinuous peptide within the A chain’s loop region. Previous research has emphasized the immunological significance of the Loop region, highlighting its enhanced recognition and stimulatory impact on the immune response. Consequently, it is recommended that both the structural configuration and the sequence characteristics of the Loop region be integrated into the design of novel antibody architectures, diagnostic assays, and therapeutic antibodies [71, 72].

Supplementary Information

The online version contains supplementary material available at <https://doi.org/10.1186/s12985-024-02504-w>.

Supplementary Material 1.

Supplementary Material 2.

Acknowledgements

This work was supported by grant from National Natural Science Foundation in China (Grant No. 32071476 to X.M.) and sponsored by Natural Science Foundation of Xinjiang Uygur Autonomous Region (Project No.2022D01A324).

Author contributions

X.M. and K.Y. conceived the study. K.Y., Z.W., X.W., M.B., S.H., K.L., X.P., Y.W. and D.M. performed the experiments. K.Y. wrote the manuscript. X.M. supervised all of the research and revised the manuscript. All authors read and approved the final manuscript.

Funding

This work was supported by grant from National Natural Science Foundation in China (Grant No. 32071476 to X.M.) and sponsored by Natural Science Foundation of Xinjiang Uygur Autonomous Region (Project No.2022D01A324).

Availability of data and materials

The sequencing data obtained in this study has been uploaded to the GenBank database (accession numbers were in supplementary materials).

Declarations

Ethics approval and consent to participate

Not applicable.

Consent for publication

All authors agree to publish the research data.

Competing interests

The authors declare no competing interests.

Received: 15 May 2024 Accepted: 14 September 2024

Published online: 27 September 2024

References

- Opriessnig T, Karuppannan AK, Castro A, Xiao CT. Porcine circoviruses: current status, knowledge gaps and challenges. *Virus Res*. 2020;286:198044.
- Cao L, Sun W, Lu H, Tian M, Xie C, Zhao G, et al. Genetic variation analysis of PCV1 strains isolated from Guangxi Province of China in 2015. *BMC Vet Res*. 2018;14(1):43.
- Tischer I, Gelderblom H, Vettermann W, Koch MA. A very small porcine virus with circular single-stranded DNA. *Nature*. 1982;295(5844):64–6.
- Allan GM, McNeilly F, Kennedy S, Daft B, Clarke EG, Ellis JA, et al. Isolation of porcine circovirus-like viruses from pigs with a wasting disease in the USA and Europe. *J Vet Diagn Invest*. 1998;10(1):3–10.
- Davies B, Wang X, Dvorak CM, Marthaler D, Murtaugh MP. Diagnostic phylogenetics reveals a new Porcine circovirus 2 cluster. *Virus Res*. 2016;217:32–7.
- Segales J, Olvera A, Grau-Roma L, Charreyre C, Nauwincq H, Larsen L, et al. PCV-2 genotype definition and nomenclature. *Vet Rec*. 2008;162(26):867–8.
- Franzo G, Segales J. Porcine circovirus 2 (PCV-2) genotype update and proposal of a new genotyping methodology. *PLoS ONE*. 2018;13(12):e0208585.
- Vargas-Bermudez DS, Mogollon JD, Jaime J. The prevalence and genetic diversity of PCV3 and PCV2 in Colombia and PCV4 Survey during 2015–2016 and 2018–2019. *Pathogens*. 2022;11(6).
- Jia Y, Zhu Q, Xu T, Chen X, Li H, Ma M, et al. Detection and genetic characteristics of porcine circovirus type 2 and 3 in Henan Province of China. *Mol Cell Probes*. 2022;61:101790.
- Darwich L, Mateu E. Immunology of porcine circovirus type 2 (PCV2). *Virus Res*. 2012;164(1–2):61–7.
- Meng XJ. Porcine circovirus type 2 (PCV2): pathogenesis and interaction with the immune system. *Annu Rev Anim Biosci*. 2013;1:43–64.
- Opriessnig T, Meng XJ, Halbur PG. Porcine circovirus type 2 associated disease: update on current terminology, clinical manifestations, pathogenesis, diagnosis, and intervention strategies. *J Vet Diagn Invest*. 2007;19(6):591–615.
- Phan TG, Giannitti F, Rossow S, Marthaler D, Knutson TP, Li L, et al. Detection of a novel circovirus PCV3 in pigs with cardiac and multi-systemic inflammation. *Virol J*. 2016;13(1):184.
- Fu X, Fang B, Ma J, Liu Y, Bu D, Zhou P, et al. Insights into the epidemic characteristics and evolutionary history of the novel porcine circovirus type 3 in Southern China. *Transbound Emerg Dis*. 2018;65(2):e296–303.
- Zhai SL, Zhou X, Zhang H, Hause BM, Lin T, Liu R, et al. Comparative epidemiology of porcine circovirus type 3 in pigs with different clinical presentations. *Virol J*. 2017;14(1):222.
- Palinski R, Pineyro P, Shang P, Yuan F, Guo R, Fang Y et al. A novel porcine circovirus distantly related to known circoviruses is associated

- with porcine dermatitis and nephropathy syndrome and reproductive failure. *J Virol.* 2017;91(1).
17. Zhang HH, Hu WQ, Li JY, Liu TN, Zhou JY, Opriessnig T, et al. Novel circovirus species identified in farmed pigs designated as porcine circovirus 4, Hunan province, China. *Transbound Emerg Dis.* 2020;67(3):1057–61.
 18. Chen N, Xiao Y, Li X, Li S, Xie N, Yan X, et al. Development and application of a quadruplex real-time PCR assay for differential detection of porcine circoviruses (PCV1 to PCV4) in Jiangsu Province of China from 2016 to 2020. *Transbound Emerg Dis.* 2021;68(3):1615–24.
 19. Xu T, Zhang YH, Tian RB, Hou CY, Li XS, Zheng LL, et al. Prevalence and genetic analysis of porcine circovirus type 2 (PCV2) and type 3 (PCV3) between 2018 and 2020 in central China. *Infect Genet Evol.* 2021;94:105016.
 20. Wei C, Zhang M, Chen Y, Xie J, Huang Z, Zhu W, et al. Genetic evolution and phylogenetic analysis of porcine circovirus type 2 infections in southern China from 2011 to 2012. *Infect Genet Evol.* 2013;17:87–92.
 21. Sun W, Du Q, Han Z, Bi J, Lan T, Wang W, et al. Detection and genetic characterization of porcine circovirus 4 (PCV4) in Guangxi, China. *Gene.* 2021;773:145384.
 22. Mengfan Q, Xifeng W, Guowu Z, Qingling M, Jun Q, Lixia W, et al. Molecular detection and genetic diversity of porcine circovirus type 3 in commercial pig farms in Xinjiang Province, China. *J Vet Res.* 2019;63(4):481–8.
 23. Bardou P, Mariette J, Escudie F, Djemiel C, Klopp C. Jvenn: an interactive Venn diagram viewer. *BMC Bioinform.* 2014;15(1):293.
 24. Mahe D, Blanchard P, Truong C, Arnauld C, Le Cann P, Cariolet R, et al. Differential recognition of ORF2 protein from type 1 and type 2 porcine circoviruses and identification of immunorelevant epitopes. *J Gen Virol.* 2000;81(Pt 7):1815–24.
 25. Kweon CH, Nguyen LT, Yoo MS, Kang SW. Differential recognition of the ORF2 region in a complete genome sequence of porcine circovirus type 2 (PCV2) isolated from boar bone marrow in Korea. *Gene.* 2015;569(2):308–12.
 26. Lekcharoensuk P, Morozov I, Paul PS, Thangthumniyom N, Wajjawkul W, Meng XJ. Epitope mapping of the major capsid protein of type 2 porcine circovirus (PCV2) by using chimeric PCV1 and PCV2. *J Virol.* 2004;78(15):8135–45.
 27. Zheng G, Lu Q, Wang F, Xing G, Feng H, Jin Q, et al. Phylogenetic analysis of porcine circovirus type 2 (PCV2) between 2015 and 2018 in Henan Province, China. *BMC Vet Res.* 2020;16(1):6.
 28. Yu W, Zhan Y, Xue B, Dong Y, Wang Y, Jiang P, et al. Highly efficient cellular uptake of a cell-penetrating peptide (CPP) derived from the capsid protein of porcine circovirus type 2. *J Biol Chem.* 2018;293(39):15221–32.
 29. Chen HC, Chiou ST, Zheng JY, Yang SH, Lai SS, Kuo TY. The nuclear localization signal sequence of porcine circovirus type 2 ORF2 enhances intracellular delivery of plasmid DNA. *Arch Virol.* 2011;156(5):803–15.
 30. Liu J, Wei C, Dai A, Lin Z, Fan K, Fan J, et al. Detection of PCV2e strains in Southeast China. *PeerJ.* 2018;6:e4476.
 31. Kolaskar AS, Tongaonkar PC. A semi-empirical method for prediction of antigenic determinants on protein antigens. *FEBS Lett.* 1990;276(1–2):172–4.
 32. Abesamis LMI, Aliping EGA, Armada F, Danao MF, Del Valle PDB, Regencia ZJG et al. In Silico comparative analysis of predicted B cell epitopes against Dengue Virus (serotypes 1–4) isolated from the Philippines. *Vaccines (Basel).* 2022;10(8).
 33. Almalki S, Beigh S, Akhter N, Alharbi RA. In silico epitope-based vaccine design against influenza a neuraminidase protein: computational analysis established on B- and T-cell epitope predictions. *Saudi J Biol Sci.* 2022;29(6):103283.
 34. Darvishi F, Ganji A, Khansarinejad B, Sadoogh Abbasian S, Abtahi H. Cloning, expression and purification of antigenic fragments of the *Ureaplasma urealyticum* UreD protein and its value in serology. *Iran J Microbiol.* 2022;14(6):813–9.
 35. Chou PY, Fasman GD. Prediction of the secondary structure of proteins from their amino acid sequence. *Adv Enzymol Relat Areas Mol Biol.* 1978;47:45–148.
 36. Emini EA, Hughes JV, Perlow DS, Boger J. Induction of hepatitis a virus-neutralizing antibody by a virus-specific synthetic peptide. *J Virol.* 1985;55(3):836–9.
 37. Parker JM, Guo D, Hodges RS. New hydrophilicity scale derived from high-performance liquid chromatography peptide retention data: correlation of predicted surface residues with antigenicity and x-ray-derived accessible sites. *Biochemistry.* 1986;25(19):5425–32.
 38. Vihinen M. Relationship of protein flexibility to thermostability. *Protein Eng.* 1987;1(6):477–80.
 39. Karplus PA, Schulz GE. Prediction of chain flexibility in proteins. *Naturwissenschaften.* 1985;72(4):212–3.
 40. Zhao Q. Protein flexibility as a biosignal. *Crit Rev Eukaryot Gene Expr.* 2010;20(2):157–70.
 41. Jespersen MC, Peters B, Nielsen M, Marcatili P. BepiPred-2.0: improving sequence-based B-cell epitope prediction using conformational epitopes. *Nucleic Acids Res.* 2017;45(W1):W24–9.
 42. Chang CC, Wu CY, Ciou JG, Wu CW, Wang YC, Chang HW, et al. Exploring the surface epitope and nuclear localization analysis of porcine circovirus type 3 capsid protein. *AMB Express.* 2023;13(1):141.
 43. Jiang M, Guo J, Zhang G, Jin Q, Liu Y, Jia R, et al. Fine mapping of linear B cell epitopes on capsid protein of porcine circovirus 3. *Appl Microbiol Biotechnol.* 2020;104(14):6223–34.
 44. Ponomarenko J, Bui HH, Li W, Füsseder N, Bourne PE, Sette A, et al. ElliPro: a new structure-based tool for the prediction of antibody epitopes. *BMC Bioinform.* 2008;9:514.
 45. Bi M, Li X, Zhai W, Yin B, Tian K, Mo X. Structural insight into the type-specific epitope of porcine circovirus type 3. *Biosci Rep.* 2020;40(6).
 46. Zheng S, Shi J, Wu X, Peng Z, Xin C, Zhang L, et al. Presence of Torque teno sus virus 1 and 2 in porcine circovirus 3-positive pigs. *Transbound Emerg Dis.* 2018;65(2):327–30.
 47. Xu T, Hou CY, Zhang YH, Li HX, Chen XM, Pan JJ, et al. Simultaneous detection and genetic characterization of porcine circovirus 2 and 4 in Henan Province of China. *Gene.* 2022;808:145991.
 48. Ouyang T, Zhang X, Liu X, Ren L. Co-infection of Swine with Porcine Circovirus Type 2 and other Swine viruses. *Viruses.* 2019;11(2).
 49. Sinha A, Shen HG, Schalk S, Beach NM, Huang YW, Meng XJ, et al. Porcine reproductive and respiratory syndrome virus (PRRSV) influences infection dynamics of porcine circovirus type 2 (PCV2) subtypes PCV2a and PCV2b by prolonging PCV2 viremia and shedding. *Vet Microbiol.* 2011;152(3–4):235–46.
 50. Zhai SL, Chen SN, Wei ZZ, Zhang JW, Huang L, Lin T, et al. Co-existence of multiple strains of porcine circovirus type 2 in the same pig from China. *Virol J.* 2011;8:517.
 51. Harding JC, Ellis JA, McIntosh KA, Krakowka S. Dual heterologous porcine circovirus genogroup 2a/2b infection induces severe disease in germ-free pigs. *Vet Microbiol.* 2010;145(3–4):209–19.
 52. Huang Y, Shao M, Xu X, Zhang X, Du Q, Zhao X, et al. Evidence for different patterns of natural inter-genotype recombination between two PCV2 parental strains in the field. *Virus Res.* 2013;175(1):78–86.
 53. Opriessnig T, Gauger PC, Faaberg KS, Shen H, Beach NM, Meng XJ, et al. Effect of porcine circovirus type 2a or 2b on infection kinetics and pathogenicity of two genetically divergent strains of porcine reproductive and respiratory syndrome virus in the conventional pig model. *Vet Microbiol.* 2012;158(1–2):69–81.
 54. Genzow M, Schwartz K, Gonzalez G, Anderson G, Chittick W. The effect of vaccination against porcine reproductive and respiratory syndrome virus (PRRSV) on the porcine circovirus-2 (PCV-2) load in porcine circovirus associated disease (PCVAD) affected pigs. *Can J Vet Res.* 2009;73(2):87–90.
 55. Meiners C, Loesken S, Doebering S, Starick E, Pesch S, Maas A, et al. Field study on swine influenza virus (SIV) infection in weaner pigs and sows. *Tierarztl Prax Ausg G Grosstiere Nutztiere.* 2014;42(6):351–9.
 56. Wei H, Lenz SD, Van Alstine WG, Stevenson GW, Langohr IM, Pogranichny RM. Infection of cesarean-derived colostrum-deprived pigs with porcine circovirus type 2 and swine influenza virus. *Comp Med.* 2010;60(1):45–50.
 57. Jung K, Kim J, Ha Y, Choi C, Chae C. The effects of transplacental porcine circovirus type 2 infection on porcine epidemic diarrhoea virus-induced enteritis in preweaning piglets. *Vet J.* 2006;171(3):445–50.
 58. Beach NM, Meng XJ. Efficacy and future prospects of commercially available and experimental vaccines against porcine circovirus type 2 (PCV2). *Virus Res.* 2012;164(1–2):33–42.

59. Wang F, Guo X, Ge X, Wang Z, Chen Y, Cha Z, et al. Genetic variation analysis of Chinese strains of porcine circovirus type 2. *Virus Res.* 2009;145(1):151–6.
60. Opriessnig T, O'Neill K, Gerber PF, de Castro AM, Gimenez-Lirola LG, Beach NM, et al. A PCV2 vaccine based on genotype 2b is more effective than a 2a-based vaccine to protect against PCV2b or combined PCV2a/2b viremia in pigs with concurrent PCV2, PRRSV and PPV infection. *Vaccine.* 2013;31(3):487–94.
61. Toplak I, Lazic S, Lupulovic D, Prodanov-Radulovic J, Becskei Z, Dosen R, et al. Study of the genetic variability of porcine circovirus type 2 detected in Serbia and Slovenia. *Acta Vet Hung.* 2012;60(3):409–20.
62. Jiang CG, Wang G, Tu YB, Liu YG, Wang SJ, Cai XH, et al. Genetic analysis of porcine circovirus type 2 in China. *Arch Virol.* 2017;162(9):2715–26.
63. Xiao CT, Halbur PG, Opriessnig T. Global molecular genetic analysis of porcine circovirus type 2 (PCV2) sequences confirms the presence of four main PCV2 genotypes and reveals a rapid increase of PCV2d. *J Gen Virol.* 2015;96(Pt 7):1830–41.
64. Xiao CT, Harmon KM, Halbur PG, Opriessnig T. PCV2d-2 is the predominant type of PCV2 DNA in pig samples collected in the U.S. during 2014–2016. *Vet Microbiol.* 2016;197:72–7.
65. Faustini G, Tucciarone CM, Legnardi M, Grassi L, Berto G, Drigo M, et al. Into the backyard: multiple detections of PCV-2e in rural pig farms of Northern Italy. An unexpected ecological niche? *Prev Vet Med.* 2023;216:105943.
66. Zhan Y, Yu W, Cai X, Lei X, Lei H, Wang A et al. The Carboxyl Terminus of the Porcine Circovirus type 2 capsid protein is critical to Virus-Like Particle Assembly, Cell Entry, and propagation. *J Virol.* 2020;94(9).
67. Ji W, Zhang X, Niu G, Chen S, Li X, Yang L, et al. Expression and immunogenicity analysis of the capsid proteins of porcine circovirus types 2 to 4. *Int J Biol Macromol.* 2022;218:828–38.
68. Park Y, Min K, Kim NH, Kim JH, Park M, Kang H, et al. Porcine circovirus 2 capsid protein produced in *N. benthamiana* forms virus-like particles that elicit production of virus-neutralizing antibodies in guinea pigs. *N Biotechnol.* 2021;63:29–36.
69. Kekarainen T, Segales J. Porcine circovirus 2 immunology and viral evolution. *Porcine Health Manag.* 2015;1:17.
70. Guo J, Hou L, Zhou J, Wang D, Cui Y, Feng X et al. Porcine circovirus type 2 vaccines: commercial application and research advances. *Viruses.* 2022;14(9).
71. Kelow SP, Adolf-Bryfogle J, Dunbrack RL. Hiding in plain sight: structure and sequence analysis reveals the importance of the antibody DE loop for antibody-antigen binding. *MAbs.* 2020;12(1):1840005.
72. Chang HJ, Jian JW, Hsu HJ, Lee YC, Chen HS, You JJ, et al. Loop-sequence features and stability determinants in antibody variable domains by high-throughput experiments. *Structure.* 2014;22(1):9–21.

Publisher's note

Springer Nature remains neutral with regard to jurisdictional claims in published maps and institutional affiliations.